Salinity and Water Cycle: Spatial patterns and variability of near-surface salinity gradients from historical CTD, TSG, and Argo data

Oleg Melnichenko[1] (oleg@hawaii.edu), Nikolai Maximenko[1], James Potemra[1,2], and Peter Hacker[2,3]

[1] IPRC/SOEST, University of Hawaii, Honolulu, Hawaii, [2] Hawaii Institute of Geophysics and Planetology, SOEST, University of Hawaii, [3]Physical Oceanography Program, NASA Headquarters, Washington DC

WCRP OSC
24-28 October 2011
Denver, CO

1. Abstract

Sea surface salinity (SSS) is an important variable that reflects the intensity of the marine hydrological cycle [US CLIVAR Salinity Working group, 2008]. The Aquarius satellite mission will provide, for the first time, both global and continuous observations of SSS with space and time resolution not accessible by other components of the ocean observing system. Among these components, the Argo float array is, perhaps, the most compatible due to its continuous global coverage, yet, Argo measurements are absent above 5 m depth thus leaving the most active near-surface ocean layer unobserved. As a step towards the synergy between the satellite and the sea-based observations, we analyze near-surface salinity gradients in historical data sets.

This way, open ocean data of high-resolution CTD profiles collected in the World Ocean Database 2009 are used to characterize vertical salinity gradients. Globally, the mean value and standard deviation of the difference between salinity at 5 m depth level and SSS do not exceed 0.03 psu and 0.2 psu, respectively. At the same time, probability distribution of this difference is strongly skewed towards positive values due to relatively rare events of anomalously low SSS. Using the statistics gained from the analysis of historical CTD casts, the Argo data are then utilized to reconstruct seasonal maps of probability of appearance of a complex vertical structure of salinity in the near-surface layer. The areas of high probability indicate the areas where the Aquarius mission is expected to add fundamentally new information for climate and ocean research. A struggle between precipitation and vertical mixing, which appears to be responsible for the observed evolution of the complexity of the near-surface salinity structure, is also discussed on a seasonal basis.

Horizontal near-surface salinity gradients are studied using high-resolution thermosalinograph (TSG) data, collected by the Global Ocean Surface Underway Data Pilot Project (GOSUD). Wavenumber power density spectra of SSS are then computed to determine spatial decorrelation scales as well as other statistical parameters required (e.g.) for optimal interpolation of the high-resolution SSS data, and to assess errors due to components of variability not resolved by the Aquarius measurements. A particular focus of this study is on the North Atlantic subtropical SSS maximum, where the Salinity Processes in the Upper Ocean Regional Study (SPURS) experiment is about to start.

2. Vertical gradients of salinity in the near-surface layer

2.1 Historical CTD data

To characterize salinity differences in the uppermost ocean layer we use high-resolution CTD data collected as part of the World Ocean Circulation Experiment (WOCE). The WOCE CTD data are known to be carefully calibrated by accompanying bottle samples, resulting in unprecedented accuracy of 0.002ºC for temperature and 0.002 psu for salinity (Saunders et al., 1991).

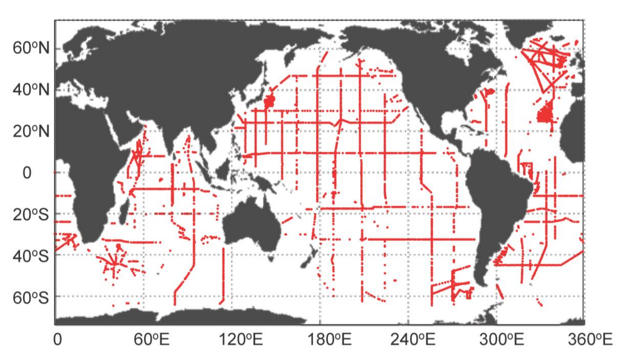

Figure 1. Locations of CTD casts with valid surface (0-1m depth) temperature and salinity measurements from WOCE data archive. Stations located within approximately 200 km distance off the nearest coast were excluded from the analysis. The selection of WOCE data is also made according to provided quality flags. Only profiles with good data (quality flag=2) are retained.

For each vertical profile:

$$\Delta S_{z_i - z_{i-1}} = S(z_i) - S(z_{i-1})$$
$$\Delta T_{z_i - z_{i-1}} = T(z_i) - T(z_{i-1})$$
$$\Delta \rho_{z_i - z_{i-1}} = \rho(z_i) - \rho(z_{i-1})$$

S - salinity (psu),

T - temperature (ºC)

ρ - density (kg/m³)

z_i - depth: [0,1]m; [4,6]m; [9-11]m.

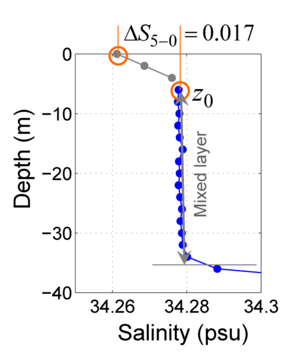

Table 1. Statistics of ΔS_{5-0}

WOCE	profiles	mean (psu)	std (psu)	skew
all data (flag=2)	5635	0.021	0.145	14.8
Tropics 22ºS -22ºN	1934	0.028	0.157	12.4
Off tropics	3701	0.016	0.126	16.3

Over the whole dataset, the mean and standard deviation of ΔS_{5-0} are equal 0.021 and 0.15 psu, respectively. Probability distributions of ΔS_{5-0} are severely skewed toward positive values due to anomalous low-salinity measurements at the surface (Table 1).

Table 2. Statistics of ΔS_{5-0} for different sub-sets of CTD data

WOCE	profiles	mean (psu)	std (psu)	skew
All data	5635	0.021	0.145	14.8
$\Delta S_{10-5} < 0.02$	5226	0.016	0.131	16.4
$\Delta S_{10-5} \geq 0.02$	409	0.075	0.186	4.7

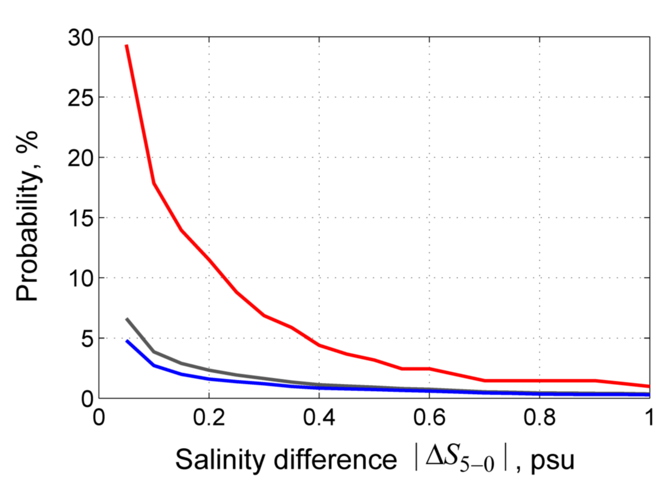

Figure 2. Probability, P (%), that the difference between salinity at 5 m depth and SSS, $|\Delta S_{5-0}|$, is larger than or equal to a prescribed threshold, calculated for three distinct groups of CTD profiles. Some statistical characteristics of the near-surface salinity differences for each group of profiles are provided in Table 2. Colors of numbers in Table 2 correspond to those of curves in Fig. 2. Over the whole dataset, only about 6% of CTD profiles exhibit near-surface salinity differences larger than or equal to 0.1 psu (black curve). However, CTD profiles, which exhibit relatively large salinity difference between 10 m and 5 m depth, are also more likely to show large values of the near-surface salinity difference (red curve).

2.2 Argo data

Unlike historical CTD data, the Argo float array provides global coverage with high density of observations in both time and space. Although Argo observations are limited to layers at and below 5 m depth, combined with statistics inferred from the analysis of historical CTD data, they appear to be useful for characterizing regions where and when discrepancies between *in situ* salinity measurements and Aquarius SSS retrievals are expected to be significant.

Consider, for example, two groups of Argo profiles, one of which combines all profiles that have a signature of a 'complex' vertical structure of salinity in the near-surface layer, |S(10m)-S(5m)|>0.02 psu, and the other group combines 'simple' profiles, characterized by well mixed salinity in the near-surface layer, |S(10m)-S(5m)|<0.02 psu. Since these two groups of profiles are mutually exclusive (two events cannot occur at the same time), probability of occurrence of a 'complex' salinity structure in the near-surface layer can readily be calculated from the statistics of Argo floats.

$A: |\Delta S_{10-5}| < 0.02$ psu, $B: |\Delta S_{10-5}| \geq 0.02$ psu; $P_B = N_B/(N_A + N_B)$, $P_A = 1 - P_B$, N - number of profiles in a 10º×10º bin

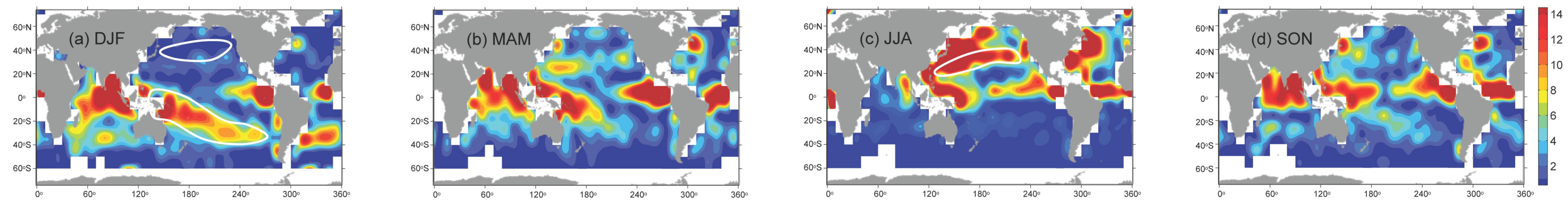

Figure 3. Probability, P_B (%), of appearance of a complex vertical structure of salinity in the near-surface ocean layer. The areas of high probability indicate the areas where the Aquarius mission is expected to add fundamentally new information for climate and ocean research. Alternatively, the areas of low probability indicate the areas, which are most suitable for the Aquarius calibration and validation. The maps are smoothed for better visualization. Bins with less than 70 profiles are blanked.

It is also instructive to compare seasonal patterns of probability of occurrence of a complex vertical structure of salinity in the near-surface layer with those of some forcing agents, responsible for the evolution of the upper ocean mixed layer:

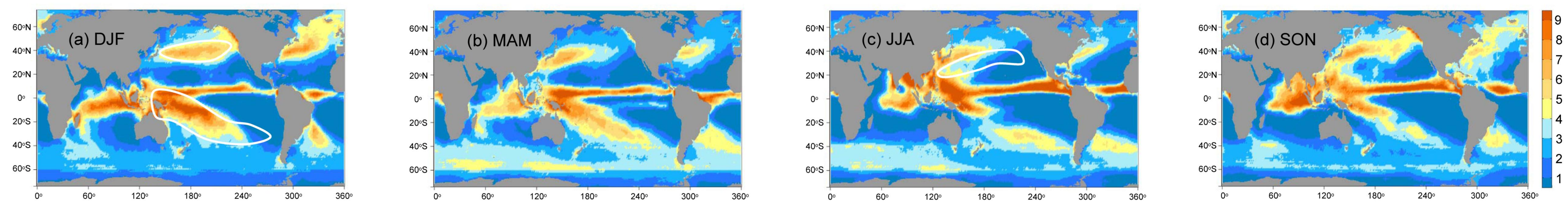

Figure 4. Seasonal mean precipitation (mm/day), calculated from GPCP daily data (2001-2009).

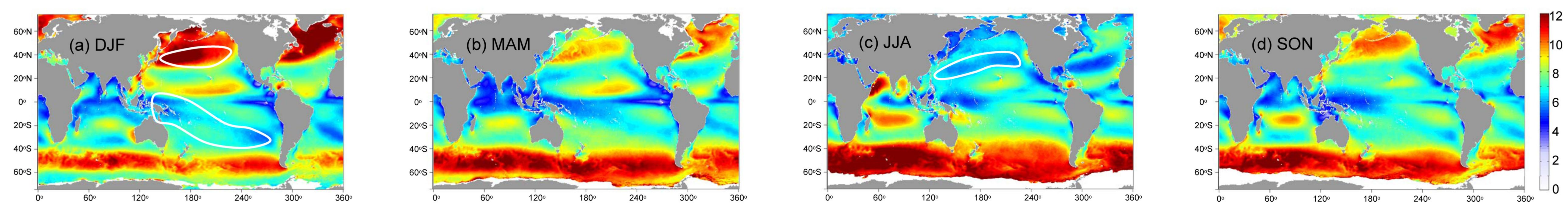

Figure 5. Seasonal mean QuikSCAT wind speed (m/sec).

The geographical distribution of probability of occurrence of a complex vertical structure of salinity in the near-surface ocean layer (Fig. 3) is highly heterogeneous, vary seasonally, and reflects a struggle between precipitation and the mixing action of the wind. In boreal winter, for example, the tilted tongue of high probability (Fig. 3a) coincides with a region of high precipitation associated with the South Pacific convergence zone (Fig. 4a). This region is also characterized by relatively low near-surface winds (Fig. 5a). In the North Pacific, however, the vast area of high precipitation is largely compensated by the mixing effect of strong winds, resulting in low probability of appearance of a complex salinity structure in the near-surface ocean layer.

This is further confirmed by comparing Fig. 3 and Fig. 6; the latter is probability of occurrence of a shallow mixed layer (A: MLD >15 m, B: MLD≤ 15 m)

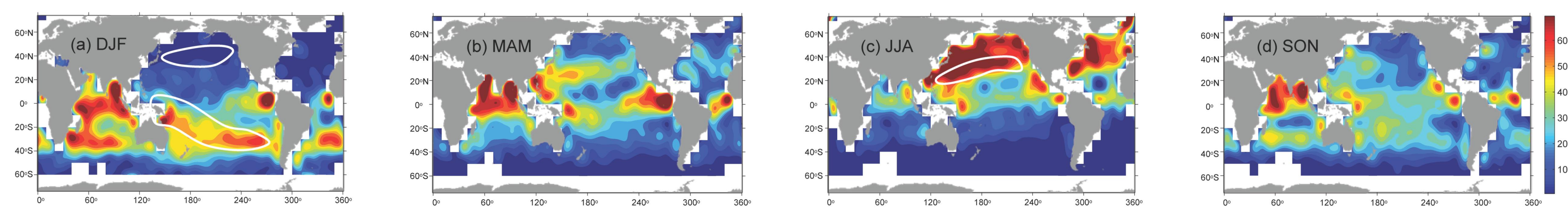

Figure 6. Probability that the mixed layer depth, as seen by Argo floats, is shallower than 15 m depth. A search for the mixed layer depth for each Argo profile was conducted using the potential density threshold of 0.02 kg m⁻³.

3. Spatial variability (subtropical North Atlantic)

Used are high-resolution (dr<4 km) TSG lines, collected by the GOSUD project:

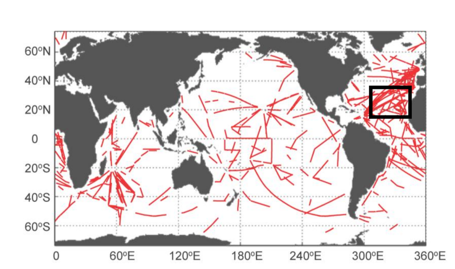

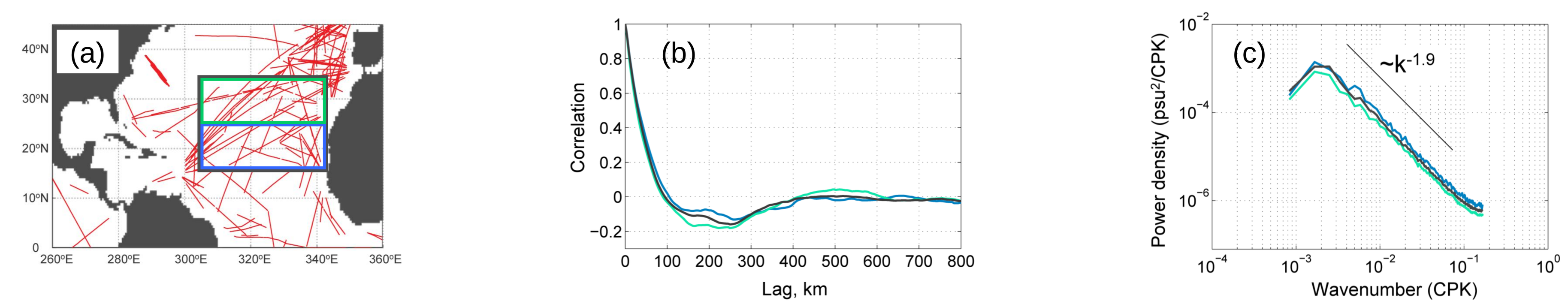

Figure 7. (a) High-resolution TSG lines selected for the analysis; (b) Mean autocorrelation functions evaluated in three sub-domains shown in (a); and (c) the corresponding wavenumber spectra.

As seen from the spectra (Fig. 7c), there are no significant differences between the two regions. In the wavelength range from 15 km to about 400 km, the spectra follow a power law of the form ~k^{-n}. The the value of *n* characterizes the spatial distribution of SSS. We find that in the subtropical North Atlantic the slope of the SSS spectrum is *n*=-1.9, which is much steeper than theoretical arguments of 2D turbulent flow predict (*n*=-1, assuming that SSS is a passive tracer). The observed *n* indicates that the small-scale structures are less energetic than expected and the spatial gradients of SSS reflect primarily the scale of large coherent vortices. Indeed, the first zero crossing of the correlation function is L_0=100 km (Fig. 7b), which is consistent with the length scale of the energy containing eddies in this region [Eden, 2007; Chelton et al., 2007, 2011].

Acknowledgments. We thank NASA Physical Oceanography Program for financial support of this study through grant NNX09AU75G . IPRC is partly supported by the Japan Agency for Marine-Earth Science and Technology (JAMSTEC), by NASA through grant No. NNX07AG53G, and by NOAA through grant No. NA09OAR4320075 . We acknowledge the use of freely available Argo data collected by the International Argo Project and the national programs that contribute to it (http://www.argo.ucsd.edu). We thank the GOSUD Project (http://www.gosud.org) for providing free access to the TSG data.